Ergodic Capacity Performance of NOMA-SWIPT Aided IoT Relay Systems with Direct Link

Ashish Rauniyar[†*], Paal Engelstad[†*], Olav N. Østerbø[‡]
[†]Department of Technology Systems, University of Oslo, Norway
[*]Department of Computer Science, OsloMet - Oslo Metropolitan University, Norway
[‡]Telenor Research, Norway
Email: (ashish.rauniyar, paal.engelstad)@oslomet.no, olav.osterbo@getmail.no

***Abstract*—For the delay-tolerant transmission mode, ergodic capacity (EC) is an appropriate measure for the performance analysis of the system. In this paper, we investigate the EC and ergodic sum capacity (ESC) performance of cooperative non-orthogonal multiple access (NOMA) simultaneous wireless information and power transfer (SWIPT) aided Internet of Things (IoT) relay systems with direct links over the Rayleigh fading channels. To the best of our knowledge, there is no published literature that investigates the EC and ESC of the NOMA-SWIPT aided IoT relay systems with the direct link, in which one source or base station (BS) transmits symbol to two destination nodes through the direct link and with the help of EH based relay node. Specifically, we study the time switching (TS), and power splitting (PS) relaying architecture for increasing the spectral and energy-efficiency of the considered system. Analytical expressions for the EC and the ESC are mathematically derived and validated by the simulation results. Our results not only provide a thorough comparison of the TS and PS relaying EH architecture for the considered system model, but it also demonstrates that the ESC performance could be significantly improved through the optimal choice of the power splitting ϵ factor for PS relaying with NOMA compared to TS relaying with NOMA.**

***Index Terms*—Internet of Things, Energy Harvesting, NOMA, Direct link, SWIPT, Ergodic capacity.**

I. Introduction

With the emergence of the Internet of Things (IoT), the fifth-generation (5G) and the next-generation cellular networks is expected to support the massive connectivity of the IoT devices [1]. In this regard, non-orthogonal multiple access (NOMA) has been contemplated as a promising radio access technique for the 5G and next-generation networks [2] [3] [4]. In particular, in the power domain (PD) NOMA, multiple users' signals are superimposed in the PD so that signals of multiple users can be transmitted in the same frequency, time, and code [5]. Specifically, multiple users are allocated with different power levels according to their perceived channel conditions. Users with strong channel conditions are allocated less power, and it first decodes the signal of the user with weak channel conditions by considering its own signal as noise and then it decodes its signal by using successive interference cancellation (SIC) technique [6].

On the other hand, sensors are the principal components that make the idea of IoT into reality. However, these sensors in the IoT devices are usually battery operated, which limits its lifetime operation. Moreover, it is difficult to replace the battery of these IoT sensor nodes if it is deployed in a hostile or hazardous environments [7]. Therefore, simultaneous wireless information and power transfer (SWIPT) is being considered as an energy-efficient viable approach for self-sustainable green communication in IoT networks [8] [9]. Due to the practical considerations of the energy harvesting (EH) circuit of the receivers, SWIPT cannot be directly applied for the information decoding (ID) at the same time. Therefore, power splitting (PS) and time switching (TS) relaying are two popular EH architectures widely considered for SWIPT. Thus, by following the signal partition method for EH and ID, in the PS relaying, the relay node splits the incoming power signal for EH and ID while in the TS relaying, a fraction of time is used for EH and ID separately [10].

Due to the high spectral efficiency of NOMA, it is being applied in conjugation with many other technologies such as cooperative relaying [11] and SWIPT [8]. An RF EH and information transmission based on TS, PS, and NOMA for wireless powered IoT relay system was studied in [12] where an IoT relay node operated in a dual-mode of energy harvesting and transmitting its own data along with the source data to their respective destination nodes. Further, the model was extended and studied by introducing the interference factor in [13]. In [12] and [13], a general assumption was made that no direct links were available in the system and hence, the data transmission was only possible through relaying. However, in wireless communication, it is known that when the direct links between the base station (BS) and the users exist and are non-negligible, consolidating direct links could significantly enhance the performance of cooperative relaying systems [14], [15]. A Decode-and-Forward (DF) relaying for a cooperative NOMA systems with direct links was analyzed in [16]. Although the authors in [16] analyzed three different relaying schemes, the EH was not considered in their system model. Analyzing and studying the impact of EH in the NOMA-SWIPT system is important as it will help us to design an energy-efficient system by providing new insight into the effect of different EH parameters in the system. Therefore, the authors in [17] studied the outage performance of EH DF relaying NOMA networks considering the direct link. However, the authors did not study the ergodic capacity (EC) for the considered system model with direct links. The reason for studying EC and ergodic sum capacity (ESC) of the system

ISBN 978-3-903176-29-4 © 2020 IFIP

is obvious and necessary. For a delay-tolerant transmission mode, the source transmits at any constant rate upper bounded by the EC. Since the length of the codeword relative to the block time is sufficiently large, the codeword could experience all possible realizations of the channel [18]. Therefore, the EC becomes an appropriate measure for the performance analysis of the system.

Therefore, motivated by the works in [16] and [17] and taking the EC as a fundamental performance indicator, in this paper, we investigate the EC performance of NOMA-SWIPT aided IoT relay systems with direct links over the Rayleigh fading channels. Specifically, for the considered NOMA-SWIPT system, we study two popular energy harvesting architecture - TS and PS relaying architecture for increasing the spectral and energy-efficiency of the system. In summary, the principle contributions of this paper are as follows:

- To the best of our knowledge, there is no published literature that investigates the EC and ESC of the NOMA-SWIPT aided IoT relay systems with direct links, in which one source or base station (BS) wants to transmit symbols to two destination nodes through the direct links and with the help of EH based relay node.
- Specifically, for the considered NOMA-SWIPT system, we investigate TSR, PSR relaying architecture.
- We derive the analytical expressions for the EC and the ESC for the considered system model and validate it through the simulation results, which shows that our derived analytical expressions are intact.
- Our results not only provide a thorough comparison of TS and PS relaying EH architecture for the considered NOMA-SWIPT system model with direct links, but it also demonstrates that the EC performance could be significantly improved through the optimal choice of power splitting ϵ factor for PS relaying with NOMA compared to TS relaying with NOMA.

The rest of the paper is organized as follows. In Section II, we explain the system model of the considered scenario. In Section III, we describe the system model based on PS and NOMA. EC and ESC analysis and its mathematical derivations for the considered system model based on PS and NOMA are carried out in Section IV. In Section V, we explain the system model based on TS and NOMA. EC and ESC analysis and its mathematical derivations for the considered system model based on TS and NOMA are carried out in Section VI. The performance comparison demonstrated through the simulations is presented in Section VII. Finally, the conclusion and future work of the paper is discussed in Section VIII.

II. System Model

Fig. 1 shows the considered cooperative NOMA-SWIPT system model with direct links. Here, a BS transmits symbols x_1 and x_2 to UE_1 and UE_2 respectively through the direct link and via the energy-constrained relay node R. As R is a power-constrained node that acts as a DF relay, it first harvests the RF energy from the BS signal using either PS or TS protocol

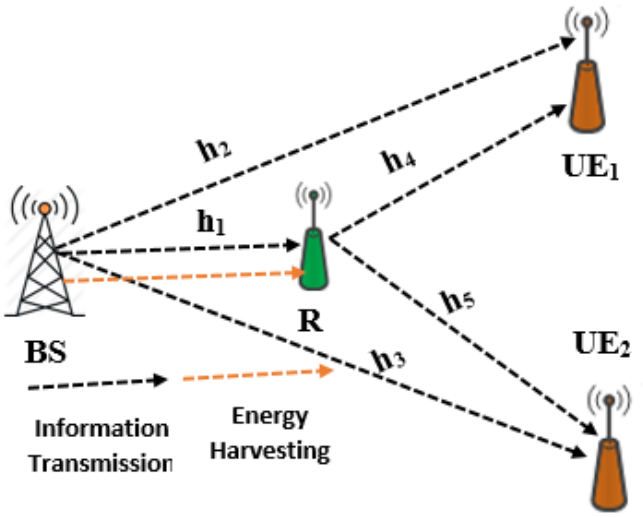

Fig. 1. Considered System Model for the NOMA-SWIPT with the Direct Link

and decodes the symbols x_1 and x_2 transmitted by the BS in the first phase. Also, UE_1 and UE_2 receives the information transmitted by the BS through the direct link in the first phase. Then, R forwards the symbol x_1 and x_2 using NOMA protocol to UE_1 and UE_2 in the next subsequent phase. We have assumed that all nodes are considered to be operating in a half-duplex mode. Each of the communication channels faces an independent Rayleigh flat fading with additive white Gaussian noise (AWGN) with zero mean and variance σ^2. The complex channel coefficient between any two nodes is denoted by $h_i \sim CN(0, \lambda_{h_i} = d_i^{-v})$ where $i \in \{1, 2, 3, 4, 5\}$, $CN(0, \lambda_{h_i} = d_i^{-v})$ is complex normal distribution to model the Rayleigh flat fading channel with zero mean variance λ_{h_i}, and d_i is the distance between the corresponding link, and v is the path loss exponent. The channel state information (CSI) is assumed to be known at all nodes. Without the loss of generality, it is assumed that $|h_1|^2 > |h_3|^2 > |h_2|^2$ and $|h_5|^2 > |h_4|^2$. Therefore, $\lambda_{h_1} > \lambda_{h_3} > \lambda_{h_2}$ and $\lambda_{h_5} > \lambda_{h_4}$. Under the availability of statistical CSI, these assumptions are an effective strategy that can be employed in the system, and it is in line with the previous work such as [11].

III. System Model based on Power Splitting (PS) and NOMA

In this scheme, the power-constrained R node first harvests the energy from the BS signal using ϵP_s, where P_s is the power of the BS transmit signal. R then uses the remaining power $(1-\epsilon)P_s$ for the information processing. The working of the system model based on PS and NOMA can be explained in two phases as:

A. First Phase

In the first phase, BS broadcast the following signal to R, UE_1 and UE_2:

$$x = \sqrt{a_1 P_s} x_1 + \sqrt{a_2 P_s} x_2 \tag{1}$$

where a_1 and a_2 are the power allocation coefficients for the symbol x_1 and x_2 respectively, and $a_1 + a_2 = 1$, $a_1 \geq a_2$.

The received signal at R, UE_1 and UE_2 can be respectively given as:

$$y_R = h_1(\sqrt{a_1 P_s} x_1 + \sqrt{a_2 P_s} x_2) + n_R \tag{2}$$

$$y_{UE_1} = h_2(\sqrt{a_1 P_s} x_1 + \sqrt{a_2 P_s} x_2) + n_{UE_1} \tag{3}$$

$$y_{UE_2} = h_3(\sqrt{a_1 P_s} x_1 + \sqrt{a_2 P_s} x_2) + n_{UE_2} \tag{4}$$

where n_R, n_{UE_1}, and $n_{UE_2} \sim CN(0, \sigma^2 = 1)$ denote the AWGN at R, UE_1, and UE_2 respectively.

Due to PS architecture at the R, the received signal in Equation 2 is split into two parts; one part is used for EH, and the other part is used for ID which can be given as [19]:

$$y_{R,EH} = h_1(\sqrt{\epsilon a_1 P_s} x_1 + \sqrt{\epsilon a_2 P_s} x_2) + n_R \tag{5}$$

$$y_{R,ID} = h_1(\sqrt{(1-\epsilon) a_1 P_s} x_1 + \sqrt{(1-\epsilon) a_2 P_s} x_2) + n_R \tag{6}$$

Now, the energy harvested at the R can be given as:

$$P_R = \eta\epsilon a_1 P_s |h_1|^2 + \eta\epsilon a_2 P_s |h_1|^2 = \eta\epsilon P_s |h_1|^2 = \eta\epsilon P_s X_1 \tag{7}$$

where $|h_1|^2 \sim X_1$.

Now, the received signal-to-noise interference ratio (SINR) for x_1 at the R, UE_1 and UE_2 can be respectively given as:

$$\gamma_R^{x_1} = \frac{a_1(1-\epsilon) P_s |h_1|^2}{a_2(1-\epsilon) P_s |h_1|^2 + \sigma^2} = \frac{a_1(1-\epsilon) P X_1}{a_2(1-\epsilon) P X_1 + 1} \tag{8}$$

$$\gamma_{UE_1}^{x_1} = \frac{a_1 P_s |h_2|^2}{a_2 P_s |h_2|^2 + \sigma^2} = \frac{a_1 P X_2}{a_2 P X_2 + 1} \tag{9}$$

$$\gamma_{UE_2}^{x_1} = \frac{a_1 P_s |h_3|^2}{a_2 P_s |h_3|^2 + \sigma^2} = \frac{a_1 P X_3}{a_2 P X_3 + 1} \tag{10}$$

where $\frac{P_s}{\sigma^2} \sim P$, $|h_2|^2 \sim X_2$ and where $|h_3|^2 \sim X_3$.

Since, R and UE_2 have better channel conditions than the UE_1, following the NOMA protocol, R and UE_2 decode the symbol x_2 by cancelling x_1 with SIC. Therefore, received SINR for x_2 at the R and UE_2 can be respectively given as:

$$\gamma_R^{x_2} = a_2(1-\epsilon) P |h_1|^2 = a_2(1-\epsilon) P X_1 \tag{11}$$

$$\gamma_{UE_2}^{x_2} = a_2 P |h_3|^2 = a_2 P X_3 \tag{12}$$

B. Second Phase:

In this phase, R now forwards the successfully decoded symbol x_1 and x_2 in the first phase to the UE_1 and UE_2 with the harvested energy in Equation 7 as transmit power P_R. R broadcasts the signal $(\sqrt{b_1 P_R} x_1 + \sqrt{b_2 P_R} x_2)$ to UE_1 and UE_2 with b_1 and b_2 as power allocation coefficients for the decoded symbols x_1 and x_2 respectively, and $b_1 + b_2 = 1$, $b_1 \geq b_2$.

The received signal at the UE_1 and UE_2 in the second phase can be respectively given as:

$$y_{UE_1}^{II} = h_4(\sqrt{b_1 P_R} x_1 + \sqrt{b_2 P_R} x_2) + n_{UE_1}^{II} \tag{13}$$

$$y_{UE_2}^{II} = h_5(\sqrt{b_1 P_R} x_1 + \sqrt{b_2 P_R} x_2) + n_{UE_2}^{II} \tag{14}$$

where $n_{UE_1}^{II}$, and $n_{UE_2}^{II} \sim CN(0, \sigma^2 = 1)$ denote the AWGN at UE_1, and UE_2 respectively and $|h_4|^2 \sim X_4$, $|h_5|^2 \sim X_5$.

Since, UE_1 has weaker channel conditions than the UE_2, following the NOMA protocol, UE_1 decodes x_1 by treating x_2 as noise.

$$\gamma_{UE_1}^{x_1,II} = \frac{b_1 P_R |h_4|^2}{b_2 P_R |h_4|^2 + 1} = \frac{b_1 P_R X_4}{b_2 P_R X_4 + 1} = \frac{b_1 \eta\epsilon P X_1 X_4}{b_2 \eta\epsilon P X_1 X_4 + 1} \tag{15}$$

UE_2 decodes x_2 after decoding x_1 and cancelling it through SIC.

$$\gamma_{UE_2}^{x_1,II} = \frac{b_1 P_R |h_5|^2}{b_2 P_R |h_5|^2 + 1} = \frac{b_1 P_R X_5}{b_2 P_R X_5 + 1} = \frac{b_1 \eta\epsilon P X_1 X_5}{b_2 \eta\epsilon P X_1 X_5 + 1} \tag{16}$$

$$\gamma_{UE_2}^{x_2,II} = b_2 P_R |h_5|^2 = b_2 P_R X_5 = b_2 \eta\epsilon P X_1 X_5 \tag{17}$$

IV. Ergodic Capacity and Ergodic Sum Capacity Analysis for the System Model Based on Power Splitting and NOMA

The achievable data rate of a dual-hop communication protocol is dominated by a inferior end-to-end link rate. Therefore, by using the Equations (8), (9), (10), (15) and (16), the achievable data rate of UE_1 associated with the symbol x_1 based on PS and NOMA can be given as:

$$C_{PS}^{x_1} = \frac{1}{2} \log_2 \left(1 + \min(\gamma_R^{x_1}, \gamma_{UE_1}^{x_1,II}, \gamma_{UE_2}^{x_1,II}, \gamma_{UE_1}^{x_1}, \gamma_{UE_2}^{x_1})\right) \tag{18}$$

Theorem 1: The EC of the UE_1 using PS and NOMA can be expressed as:

$$C_{PS-Ana}^{x_1} = \frac{1}{2\ln 2} \int_{\gamma=0}^{\frac{a_1}{a_2}} \frac{\lambda_{h_1}}{1+\gamma} e^{-\frac{(\lambda_{h_2}+\lambda_{h_3})\gamma}{P(a_1-\gamma a_2)}} \left(2\sqrt{\frac{(\lambda_{h_4}+\lambda_{h_5})\gamma}{\eta\epsilon P \lambda_{h_1}(b_1-\gamma b_2)}} \right.$$
$$K_1\left(2\sqrt{\frac{(\lambda_{h_4}+\lambda_{h_5})\gamma\lambda_{h_1}}{\eta\epsilon P(b_1-\gamma b_2)}}\right) - \sum_{n=0}^{\infty} \frac{(-1)^n}{n!} \lambda_{h_1}^n$$
$$\left. \left(\frac{\gamma}{(1-\epsilon)P(a_1-\gamma a_2)}\right)^{n+1} E_{n+2}\left(\frac{(\lambda_{h_4}+\lambda_{h_5})(1-\epsilon)(a_1-\gamma a_2)}{\eta\epsilon(b_1-\gamma b_2)}\right) \right) d\gamma \tag{19}$$

Proof:

$$F_\gamma(\gamma) = 1 - \Pr\left(\frac{a_1 P X_2}{a_2 P X_2 + 1} \geq \gamma\right) \Pr\left(\frac{a_1 P X_3}{a_2 P X_3 + 1} \geq \gamma\right) \times$$

$$\Pr\left(\frac{a_1(1-\epsilon)PX_1}{a_2(1-\epsilon)PX_1+1}\geq\gamma,\frac{b_1\eta\epsilon PX_1X_4}{b_2\eta\epsilon PX_1X_4+1}\geq\gamma,\right.$$
$$\left.\frac{b_1\eta\epsilon PX_1X_5}{b_2\eta\epsilon PX_1X_5+1}\geq\gamma\right)$$
$$F_\gamma(\gamma)=1-\Pr\left(X_2\geq\frac{\gamma}{P(a_1-\gamma a_2)}\right)$$
$$\Pr\left(X_3\geq\frac{\gamma}{P(a_1-\gamma a_2)}\right)\underbrace{\Pr\left(X_1\geq\frac{\gamma}{(1-\epsilon)P(a_1-\gamma a_2)},\right.}$$
$$\underbrace{\left.X_4\geq\frac{\gamma}{\eta\epsilon P(b_1-b_2\gamma)X_1},X_5\geq\frac{\gamma}{\eta\epsilon P(b_1-b_2\gamma)X_1}\right)}_{I_1}$$
$$F_\gamma(\gamma)=1-e^{-\frac{\gamma\lambda_{h_2}}{P(a_1-\gamma a_2)}}e^{-\frac{\gamma\lambda_{h_3}}{P(a_1-\gamma a_2)}}I_1$$
Conditioning I_1 on X_1, we get
$$F_\gamma(\gamma)=1-e^{-\frac{(\lambda_{h_2}+\lambda_{h_3})\gamma}{P(a_1-\gamma a_2)}}\int_{x_1=0}^{\infty}\Pr\left(x_1\geq\frac{\gamma}{(1-\epsilon)P(a_1-\gamma a_2)},\right.$$
$$\left.X_4\geq\frac{\gamma}{\eta\epsilon P(b_1-b_2\gamma)x_1},X_5\geq\frac{\gamma}{\eta\epsilon P(b_1-b_2\gamma)x_1}\right)f_{X_1}(x_1)dx_1$$
$$F_\gamma(\gamma)=1-e^{-\frac{(\lambda_{h_2}+\lambda_{h_3})\gamma}{P(a_1-\gamma a_2)}}\int_{x_1=\frac{\gamma}{(1-\epsilon)P(a_1-\gamma a_2)}}^{\infty}\Pr\left(X_4\geq\right.$$
$$\left.\frac{\gamma}{\eta\epsilon P(b_1-b_2\gamma)x_1},X_5\geq\frac{\gamma}{\eta\epsilon P(b_1-b_2\gamma)x_1}\right)f_{X_1}(x_1)dx_1$$
$$F_\gamma(\gamma)=1-e^{-\frac{(\lambda_{h_2}+\lambda_{h_3})\gamma}{P(a_1-\gamma a_2)}}\int_{x_1=\frac{\gamma}{(1-\epsilon)P(a_1-\gamma a_2)}}^{\infty}\Pr\left(X_4\geq\right.$$
$$\left.\frac{\gamma}{\eta\epsilon P(b_1-b_2\gamma)x_1}\right)\Pr\left(X_5\geq\frac{\gamma}{\eta\epsilon P(b_1-b_2\gamma)x_1}\right)f_{X_1}(x_1)dx_1$$
$$F_\gamma(\gamma)=1-e^{-\frac{(\lambda_{h_2}+\lambda_{h_3})\gamma}{P(a_1-\gamma a_2)}}\int_{x_1=\frac{\gamma}{(1-\epsilon)P(a_1-\gamma a_2)}}^{\infty}e^{-\frac{\lambda_{h_4}\gamma}{\eta\epsilon P(b_1-b_2\gamma)x_1}}\times$$
$$e^{-\frac{\lambda_{h_5}\gamma}{\eta\epsilon P(b_1-b_2\gamma)x_1}}\lambda_{h_1}e^{-\lambda_{h_1}x_1}dx_1$$
$$F_\gamma(\gamma)=1-\lambda_{h_1}e^{-\frac{(\lambda_{h_2}+\lambda_{h_3})\gamma}{P(a_1-\gamma a_2)}}\times$$
$$\int_{x_1=\frac{\gamma}{(1-\epsilon)P(a_1-\gamma a_2)}}^{\infty}e^{-\frac{(\lambda_{h_4}+\lambda_{h_5})\gamma}{\eta\epsilon P(b_1-b_2\gamma)x_1}-\lambda_{h_1}x_1}dx_1$$
$$F_\gamma(\gamma)=1-\lambda_{h_1}e^{-\frac{(\lambda_{h_2}+\lambda_{h_3})\gamma}{P(a_1-\gamma a_2)}}\times$$
$$\left(\underbrace{\int_{x_1=0}^{\infty}e^{-\frac{(\lambda_{h_4}+\lambda_{h_5})\gamma}{\eta\epsilon P(b_1-b_2\gamma)x_1}-\lambda_{h_1}x_1}dx_1}_{I_2}-\right.$$
$$\left.\underbrace{\int_{x_1=0}^{\frac{\gamma}{(1-\epsilon)P(a_1-\gamma a_2)}}e^{-\frac{(\lambda_{h_4}+\lambda_{h_5})\gamma}{\eta\epsilon P(b_1-b_2\gamma)x_1}-\lambda_{h_1}x_1}dx_1}_{I_3}\right)$$

The integral I_2 is in the form $\int_{x=0}^{\infty}e^{-\frac{\beta}{4x}-\gamma x}dx$ which can be solved using the formula in ([20], Equation 3.324.1) as: $\frac{\beta}{\gamma}K_1(\sqrt{\beta\gamma})$, where $K_1(.)$ is a first order modified Bessel function of the second kind.

Similarly, the integral I_3 is in the form $\int_{x=0}^{a}e^{-\frac{c}{x}-bx}dx$ which can be solved in the closed-form [12] as: $\sum_{n=0}^{\infty}\frac{(-1)^n}{n!}b^na^{n+1}E_{n+2}(\frac{c}{a})$ where $E_{n+2}(.)$ is exponential integral of order n+2.

Therefore, $F_\gamma(\gamma)=1-\lambda_{h_1}e^{-\frac{(\lambda_{h_2}+\lambda_{h_3})\gamma}{P(a_1-\gamma a_2)}}\left(2\sqrt{\frac{(\lambda_{h_4}+\lambda_{h_5})\gamma}{\eta\epsilon P\lambda_{h_1}(b_1-\gamma b_2)}}\right.$
$$\left.K_1\left(2\sqrt{\frac{(\lambda_{h_4}+\lambda_{h_5})\gamma\lambda_{h_1}}{\eta\epsilon P(b_1-\gamma b_2)}}\right)-\sum_{n=0}^{\infty}\frac{(-1)^n}{n!}\lambda_{h_1}^n\right.$$
$$\left.\left(\frac{\gamma}{(1-\epsilon)P(a_1-\gamma a_2)}\right)^{n+1}E_{n+2}\left(\frac{(\lambda_{h_4}+\lambda_{h_5})(1-\epsilon)(a_1-\gamma a_2)}{\eta\epsilon(b_1-\gamma b_2)}\right)\right)$$

The EC in terms of CDF $F_\gamma(\gamma)$ can be written as:
$$C_{PS-Ana}^{x_1}=\frac{1}{2\ln 2}\int_{\gamma=0}^{\infty}\frac{1}{1+\gamma}[1-F_\gamma(\gamma)]d\gamma$$
Substituting the $F_\gamma(\gamma)$ in the above equation, we get the final expression as in Equation 19.

This ends the proof of Theorem 1.

Now, by using the Equations (11), (12), and (17), the achievable data rate of the UE_2 associated with the symbol x_2 based on PS and NOMA can be given as:
$$C_{PS}^{x_2}=\frac{1}{2}\log_2\left(1+\min(\gamma_R^{x_2},\gamma_{UE_2}^{x_2,II},\gamma_{UE_2}^{x_2})\right)\qquad(20)$$

Theorem 2: The EC of the UE_2 using PS and NOMA can be expressed as:
$$C_{PS-Ana}^{x_2}=\frac{1}{2\ln 2}\int_{\gamma=0}^{\infty}\frac{\lambda_{h_1}}{1+\gamma}e^{-\frac{\lambda_{h_3}\gamma}{a_2P}}\left(2\sqrt{\frac{\lambda_{h_5}\gamma}{b_2\eta\epsilon P\lambda_{h_1}}}\right.$$
$$K_1\left(2\sqrt{\frac{\lambda_{h_1}\lambda_{h_5}\gamma}{b_2\eta\epsilon P}}\right)-\sum_{n=0}^{\infty}\frac{(-1)^n}{n!}\lambda_{h_1}^n\left(\frac{\gamma}{a_2(1-\epsilon)P}\right)^{n+1}$$
$$\left.E_{n+2}\left(\frac{\lambda_{h_5}a_2(1-\epsilon)}{b_2\eta\epsilon}\right)\right)d\gamma\qquad(21)$$

Proof:
$$F_\gamma(\gamma)=1-\Pr\left(a_2(1-\epsilon)PX_1\geq\gamma,b_2\eta\epsilon PX_1X_5\geq\gamma,\right.$$
$$\left.a_2PX_3\geq\gamma\right)$$
$$F_\gamma(\gamma)=1-\Pr\left(X_3\geq\frac{\gamma}{a_2P}\right)\Pr\left(X_1\geq\frac{\gamma}{a_2(1-\epsilon)P},\right.$$
$$\left.X_5\geq\frac{\gamma}{b_2\eta\epsilon PX_1}\right)$$
Now, Conditioning $\Pr\left(X_1\geq\frac{\gamma}{a_2(1-\epsilon)P},X_5\geq\frac{\gamma}{b_2\eta\epsilon PX_1}\right)$ **on** X_1
$$F_\gamma(\gamma)=1-e^{-\frac{\lambda_{h_3}\gamma}{a_2P}}\times$$

$$\int_{x_1=0}^{\infty} \Pr\left(x_1 \geq \frac{\gamma}{a_2(1-\epsilon)P}, X_5 \geq \frac{\gamma}{b_2\eta\epsilon P x_1}\right) f_{X_1}(x_1)dx_1$$

$$F_\gamma(\gamma) = 1 - e^{-\frac{\lambda_{h_3}\gamma}{a_2 P}} \int_{x_1=\frac{\gamma}{a_2(1-\epsilon)P}}^{\infty} \Pr\left(X_5 \geq \frac{\gamma}{b_2\eta\epsilon P x_1}\right) \times$$

$$f_{X_1}(x_1)dx_1$$

$$F_\gamma(\gamma) = 1 - \lambda_{h_1} e^{-\frac{\lambda_{h_3}\gamma}{a_2 P}} \int_{x_1=\frac{\gamma}{a_2(1-\epsilon)P}}^{\infty} e^{-\frac{\lambda_{h_5}\gamma}{b_2\eta\epsilon P x_1} - \lambda_{h_1} x_1} dx_1$$

$$F_\gamma(\gamma) = 1 - \lambda_{h_1} e^{-\frac{\lambda_{h_3}\gamma}{a_2 P}} \left(\int_{x_1=0}^{\infty} e^{-\frac{\lambda_{h_5}\gamma}{b_2\eta\epsilon P x_1} - \lambda_{h_1} x_1} dx_1 - \right.$$

$$\left. \int_{x_1=0}^{\frac{\gamma}{a_2(1-\epsilon)P}} e^{-\frac{\lambda_{h_5}\gamma}{b_2\eta\epsilon P x_1} - \lambda_{h_1} x_1} dx_1 \right)$$

$$F_\gamma(\gamma) = 1 - \lambda_{h_1} e^{-\frac{\lambda_{h_3}\gamma}{a_2 P}} \left(2\sqrt{\frac{\lambda_{h_5}\gamma}{b_2\eta\epsilon P\lambda_{h_1}}} K_1\left(2\sqrt{\frac{\lambda_{h_1}\lambda_{h_5}\gamma}{b_2\eta\epsilon P}}\right) - \right.$$

$$\left. \sum_{n=0}^{\infty} \frac{(-1)^n}{n!} \lambda_{h_1}^n \left(\frac{\gamma}{a_2(1-\epsilon)P}\right)^{n+1} E_{n+2}\left(\frac{\lambda_{h_5} a_2(1-\epsilon)}{b_2\eta\epsilon}\right) \right)$$

Now, the EC in terms of CDF $F_\gamma(\gamma)$ can be written as:

$$C_{PS-Ana}^{x_2} = \frac{1}{2\ln 2} \int_{\gamma=0}^{\infty} \frac{1}{1+\gamma}[1 - F_\gamma(\gamma)]d\gamma$$

Substituting the $F_\gamma(\gamma)$ in the above equation, we get the final expression as in Equation 21.

This ends the proof of Theorem 2.

Now, by combining the Equation (19) and Equation (21) gives the analytical expression for the Ergodic sum capacity of the considered system based on PS and NOMA with the direct link.

$$C_{ESum}^{PS} = C_{PS-Ana}^{x_1} + C_{PS-Ana}^{x_2} \tag{22}$$

It should be noted that the final analytical expression of $C_{PS-Ana}^{x_1}$ and $C_{PS-Ana}^{x_2}$ as shown in Theorem 1 and Theorem 2 contains an integral term which is difficult to evaluate in the closed form, but it can be evaluated through numerical approaches using softwares such as MATLAB or Mathematica.

V. System Model based on Time Switching and NOMA

In TS relaying scheme, power-constrained R node first harvests the energy from the BS signal for αT duration and uses the time $\frac{(1-\alpha)T}{2}$ for information decoding and $\frac{(1-\alpha)T}{2}$ for the information transmission to the UE_1 and UE_2 by following the NOMA protocol. The working of the system model based on the TS and NOMA can be explained in two phases as:

A. First Phase

In the first phase, the BS broadcast the following signal to R, UE_1 and UE_2:

$$\hat{x} = \sqrt{a_1\hat{P}_s}\hat{x_1} + \sqrt{a_2\hat{P}_s}\hat{x_2} \tag{23}$$

The received signal at the R, UE_1 and UE_2 can be respectively given as:

$$\hat{y_R} = h_1(\sqrt{a_1\hat{P}_s}\hat{x_1} + \sqrt{a_2\hat{P}_s}\hat{x_2}) + \hat{n_R} \tag{24}$$

$$\hat{y_{UE_1}} = h_2(\sqrt{a_1\hat{P}_s}\hat{x_1} + \sqrt{a_2\hat{P}_s}\hat{x_2}) + \hat{n_{UE_1}} \tag{25}$$

$$\hat{y_{UE_2}} = h_3(\sqrt{a_1\hat{P}_s}\hat{x_1} + \sqrt{a_2\hat{P}_s}\hat{x_2}) + \hat{n_{UE_2}} \tag{26}$$

The energy harvested at the R in αT period of time is given as:

$$\hat{E}_{h_{IoT_R}} = \eta\hat{P}_s|h_1|^2\alpha T, \tag{27}$$

where $0 \leq \eta \leq 1$ is the energy conversion efficiency. The transmit power of the R i.e., $\hat{P}_R$ in $\frac{(1-\alpha)T}{2}$ block of time can be given as:

$$\hat{P}_R = \frac{\hat{E}_{h_{IoT_R}}}{(1-\alpha)T/2} = \frac{2\eta\hat{P}_s|h_1|^2\alpha}{(1-\alpha)}, \tag{28}$$

Now, the SINR for $\hat{x_1}$ at the R, UE_1 and UE_2 can be respectively given as:

$$\gamma_R^{\hat{x_1}} = \frac{a_1\hat{P}_s|h_1|^2}{a_2\hat{P}_s|h_1|^2 + \sigma_R^2} = \frac{a_1\hat{P}X_1}{a_2\hat{P}X_1 + 1} \tag{29}$$

$$\gamma_{UE_1}^{\hat{x_1}} = \frac{a_1\hat{P}_s|h_2|^2}{a_2\hat{P}_s|h_2|^2 + \sigma_{UE_1}^2} = \frac{a_1\hat{P}X_2}{a_2\hat{P}X_2 + 1} \tag{30}$$

$$\gamma_{UE_2}^{\hat{x_1}} = \frac{a_1\hat{P}_s|h_3|^2}{a_2\hat{P}_s|h_3|^2 + \sigma_{UE_2}^2} = \frac{a_1\hat{P}X_3}{a_2\hat{P}X_3 + 1} \tag{31}$$

Now, R and UE_2 decode the symbol $\hat{x_2}$ by cancelling the $\hat{x_1}$ with the SIC. Therefore, the received SINR for the $\hat{x_2}$ at the R and UE_2 can be respectively given as:

$$\gamma_R^{\hat{x_2}} = a_2\hat{P}|h_1|^2 = a_2\hat{P}X_1 \tag{32}$$

$$\gamma_{UE_2}^{\hat{x_2}} = a_2\hat{P}|h_3|^2 = a_2\hat{P}X_3 \tag{33}$$

B. Second Phase:

In this phase, R now forwards the successfully decoded symbol x_1 and x_2 to the UE_1 and UE_2 with the harvested energy as shown in Equation 28 as the transmit power $\hat{P}_R$. R broadcasts the signal $(\sqrt{b_1\hat{P}_R}\hat{x_1} + \sqrt{b_2\hat{P}_R}\hat{x_2})$ to UE_1 and UE_2 with b_1 and b_2 as the power allocation coefficients for the decoded symbols $\hat{x_1}$ and $\hat{x_2}$ respectively, and $b_1 + b_2 = 1$, $b_1 \geq b_2$.

The received signal at UE_1 and UE_2 in the second phase can be respectively given as:

$$\hat{y_{UE_1}^{II}} = h_4(\sqrt{b_1\hat{P}_R}\hat{x_1} + \sqrt{b_2\hat{P}_R}\hat{x_2}) + n_{UE_1}^{II} \tag{34}$$

$$\hat{y_{UE_2}^{II}} = h_5(\sqrt{b_1\hat{P}_R}\hat{x_1} + \sqrt{b_2\hat{P}_R}\hat{x_2}) + n_{UE_2}^{II} \tag{35}$$

Now, the UE_1 decodes the $\hat{x_1}$ by treating the $\hat{x_2}$ as a noise.

$$\gamma_{UE_1}^{\hat{x_1},II} = \frac{b_1\hat{P}_R|h_4|^2}{b_2\hat{P}_R|h_4|^2 + 1} = \frac{b_1\frac{2\alpha}{(1-\alpha)}\eta\hat{P}X_1X_4}{b_2\frac{2\alpha}{(1-\alpha)}\eta\hat{P}X_1X_4 + 1} \tag{36}$$

UE_2 decodes $\hat{x_2}$ after decoding the $\hat{x_1}$ and cancelling it through SIC.

$$\gamma_{UE_2}^{\hat{x_1},II} = \frac{b_1\hat{P}_R|h_5|^2}{b_2\hat{P}_R|h_5|^2+1} = \frac{b_1\frac{2\alpha}{(1-\alpha)}\eta\hat{P}X_1X_5}{b_2\frac{2\alpha}{(1-\alpha)}\eta\hat{P}X_1X_5+1} \quad (37)$$

$$\gamma_{UE_2}^{\hat{x_2},II} = b_2\hat{P}_R|h_5|^2 = b_2\hat{P}_RX_5 = b_2\frac{2\alpha}{(1-\alpha)}\eta\hat{P}X_1X_5 \quad (38)$$

VI. Ergodic Capacity and Ergodic Sum Capacity Analysis for the System Model Based on Time Switching and NOMA

By using the Equations (29), (30), (31), (36) and (37), the achievable data rate of UE_1 associated with the symbol x_1 based on TS and NOMA can be given as:

$$C_{TS}^{x_1} = \frac{(1-\alpha)}{2}\log_2\left(1+\min(\gamma_R^{\hat{x}_1}, \gamma_{UE_1}^{\hat{x_1},II}, \gamma_{UE_2}^{\hat{x_1},II}, \gamma_{UE_1}^{\hat{x_1}}, \gamma_{UE_2}^{\hat{x_1}})\right) \quad (39)$$

Theorem 3: The EC of the UE_1 using TS and NOMA can be expressed as:

$$C_{TS-Ana}^{x_1} = \frac{(1-\alpha)}{2\ln 2}\int_{\gamma=0}^{\frac{a_1}{a_2}} \frac{\lambda_{h_1}}{1+\gamma} e^{-\frac{(\lambda_{h_2}+\lambda_{h_3})\gamma}{\hat{P}(a_1-\gamma a_2)}} \Bigg(2\sqrt{\frac{(\lambda_{h_4}+\lambda_{h_5})\gamma}{\frac{2\eta\alpha}{1-\alpha}\hat{P}\lambda_{h_1}(b_1-\gamma b_2)}} K_1\left(2\sqrt{\frac{(\lambda_{h_4}+\lambda_{h_5})\gamma\lambda_{h_1}}{\frac{2\eta\alpha}{1-\alpha}\hat{P}(b_1-\gamma b_2)}}\right) - \sum_{n=0}^{\infty}\lambda_{h_1}^n \frac{(-1)^n}{n!}\left(\frac{\gamma}{\hat{P}(a_1-\gamma a_2)}\right)^{n+1} E_{n+2}\left(\frac{(\lambda_{h_4}+\lambda_{h_5})(a_1-\gamma a_2)}{\frac{2\eta\alpha}{1-\alpha}(b_1-\gamma b_2)}\right)\Bigg) d\gamma \quad (40)$$

Proof: The proof can be derived by following the similar steps as in the proof of Theorem 1.

By using the Equations (32), (33), and (38), the achievable data rate of UE_2 associated with the symbol x_2 based on TS and NOMA can be given as:

$$C_{TS}^{x_2} = \frac{(1-\alpha)}{2}\log_2\left(1+\min(\gamma_R^{x_2}, \gamma_{UE_2}^{x_2,II}, \gamma_{UE_2}^{x_2})\right) \quad (41)$$

Theorem 4: The EC of the UE_2 using TS and NOMA can be expressed as:

$$C_{TS-Ana}^{x_2} = \frac{(1-\alpha)}{2\ln 2}\int_{\gamma=0}^{\infty} \frac{\lambda_{h_1}}{1+\gamma} e^{-\frac{\lambda_{h_3}\gamma}{a_2\hat{P}}} \Bigg(2\sqrt{\frac{\lambda_{h_5}\gamma}{\frac{2b_2\eta\alpha\hat{P}\lambda_{h_1}}{1-\alpha}}} K_1\left(2\sqrt{\frac{\lambda_{h_1}\lambda_{h_5}\gamma}{\frac{2b_2\eta\alpha\hat{P}}{1-\alpha}}}\right) - \sum_{n=0}^{\infty}\frac{(-1)^n}{n!}\lambda_{h_1}^n\left(\frac{\gamma}{a_2\hat{P}}\right)^{n+1} E_{n+2}\left(\frac{\lambda_{h_5}a_2}{\frac{2b_2\eta\alpha}{1-\alpha}}\right)\Bigg) d\gamma \quad (42)$$

Proof: The proof can be derived by following the similar steps as in the proof of Theorem 2.

Now, by combining the Equation (40) and Equation (42) gives the analytical expression for the ESC of the considered system based on TS and NOMA with the direct link.

$$C_{ESum}^{TS} = C_{TS-Ana}^{x_1} + C_{TS-Ana}^{x_2} \quad (43)$$

TABLE I
Simulation Parameters

Parameter	Symbol	Values
Mean of $\|h_1\|^2 \rightarrow X_1$	λ_{h_1}	2.5
Mean of $\|h_2\|^2 \rightarrow X_2$	λ_{h_2}	1.0
Mean of $\|h_3\|^2 \rightarrow X_3$	λ_{h_3}	1.5
Mean of $\|h_4\|^2 \rightarrow X_4$	λ_{h_4}	1.5
Mean of $\|h_5\|^2 \rightarrow X_5$	λ_{h_5}	2.0
Source Node Transmit SNR	P	0-45 dB
Energy Harvesting Efficiency	η	0.9
Power Allocation Factor for NOMA	a_1	0.8
Power Allocation Factor for NOMA	a_2	0.2
Power Allocation Factor for NOMA	b_1	0.8
Power Allocation Factor for NOMA	b_2	0.2

VII. Numerical Results and Discussions

In this section, we verify our derived mathematical analysis for the EC and ESC of the considered system with the Monte-Carlo simulation results. The simulation parameters used for the experiments are listed in Table I unless otherwise stated. We have used MATLAB for the Monte-Carlo experiments by averaging over 10^5 random realizations of Rayleigh fading channels i.e., h_1, h_2, h_3, h_4 and h_5.

In Fig. 2 and Fig. 3, we plot the EC of the UE_1 and UE_2 respectively for both TS and PS relaying with NOMA against the transmit SNR at different $\alpha = 0.3, 0.5\&0.7$ and at different $\epsilon = 0.3, 0.5\&0.7$. We observe that the EC of both UE_1 and UE_2 is an increasing function with respect to increasing in transmit SNR. Also, it is observed that the EC of UE_2 is generally higher than UE_1, especially for the 20 dB transmit SNR and above. This is expected as UE_2 has better channel conditions than that of UE_1. As we increase the α value from 0.3 to 0.7, we see that the EC decreases for both UE_1 and UE_2. But, as we increase the ϵ value from 0.3 to 0.7, the EC increases for both UE_1 and UE_2. This indicates that: (i) lower α value is efficient in increasing the EC for the TS relaying with NOMA as more time can be allocated for the data transmission and (ii) higher ϵ value is efficient in increasing the EC for PS relaying with NOMA as more power can be harvested at the R which is being utilized by the R for the data transmission.

In Fig. 4, we plot the ESC of the considered system against the TS α factor or PS ϵ factor at 10 dB, 25 dB and 40 dB transmit SNR. We observe that the ESC for both TS and PS relaying with NOMA increases, reaches up to the maximum, and then it decreases. This confirms that the ESC is a concave function that has a unique maxima at which ESC of the system is maximized. Except for the lower value of α or ϵ factor, PS relaying with NOMA outperforms the TS relaying with NOMA, and this difference is more visible as we increase the transmit SNR from 10 dB to 40 dB.

Since, the relay node R is harvesting the energy which is solely utilized for the data transmission, the energy conversion efficiency η also plays an important role in the NOMA-SWIPT system. Therefore, in Fig. 5, we plot the ESC of the system against the α or ϵ factor at different η values. For plotting the Fig. 5, the transmit SNR was kept at 40 dB. We observe a

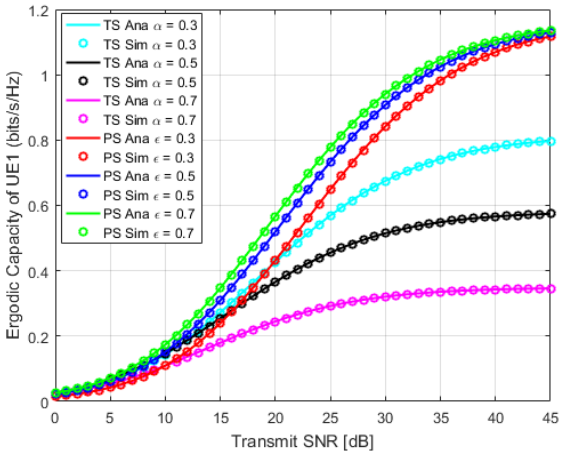

Fig. 2. Ergodic Capacity of UE1

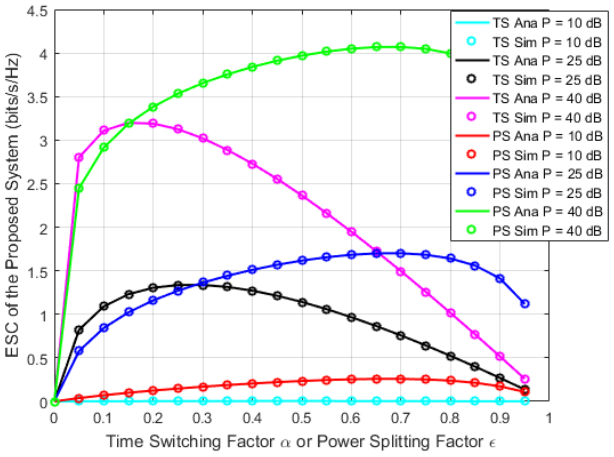

Fig. 4. Ergodic Sum Capacity v/s α or ϵ at Different P

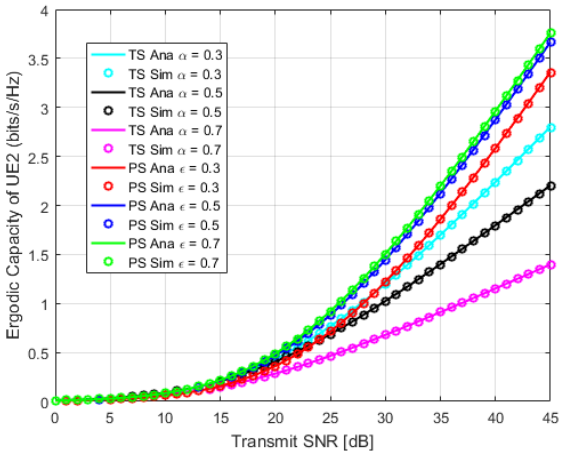

Fig. 3. Ergodic Capacity of UE2

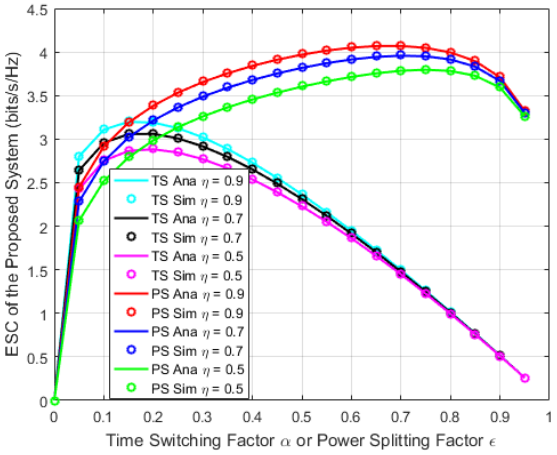

Fig. 5. Ergodic Sum Capacity v/s α or ϵ at Different η

similar pattern of the ESC performance as in Fig. 4. Moreover, as we decrease the η value, the ESC for both TS and PS relaying with NOMA decreases. This is expected as a higher η value favors the harvested energy from the signal that could be utilized for the data transmission. We also observe that as the α value increases beyond 0.65, the effect of η diminishes for the TS relaying with NOMA which confirms that smaller value of TS factor α is enough for the energy harvesting at the R.

As seen in Figures 4 and 5, there lies an optimum value of α and ϵ at which the ESC of the system is maximized. The optimal value of α and ϵ can be found out through Golden section search method as in [12]. Therefore, in Fig. 6, we found the optimal α or ϵ against different transmit SNR at two η values, 0.5 and 0.9, through the Golden section search method at which ESC of the system is maximum. We find that the optimal α values linearly decreases with the increase in the transmit SNR, whereas optimal ϵ slightly increases with the increase in transmit SNR in the beginning and after which it becomes almost saturated. This confirms that the optimal ϵ shows no positive effect with the increase in transmit SNR, unlike optimal α where the difference is clearly visible. Moreover, as expected, a higher η value such as 0.9 tends to lower the optimal α or ϵ value.

In Fig. 7, we plot the optimized ESC of the system for both TS and PS relaying with NOMA at different transmit SNR. We observe that at the lower transmit SNR values, i.e. less than 10 dB, both TS and PS relaying with NOMA almost have the same optimized ESC. After 10 dB and higher transmit SNR, PS relaying with NOMA outperforms the TS relaying with NOMA. This confirms that through the optimal choice of ϵ, it is possible to achieve better optimized ESC for the PS relaying with NOMA than the TS relaying with NOMA.

VIII. Conclusion and Future Work

EC is an appropriate measure for the performance analysis of the system. To the best of our knowledge, there is no published literature that investigates the EC and ESC of the NOMA-SWIPT aided IoT relay systems with direct links

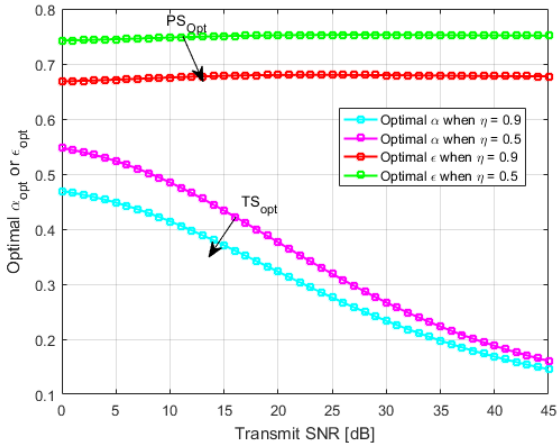

Fig. 6. Optimal α or ϵ

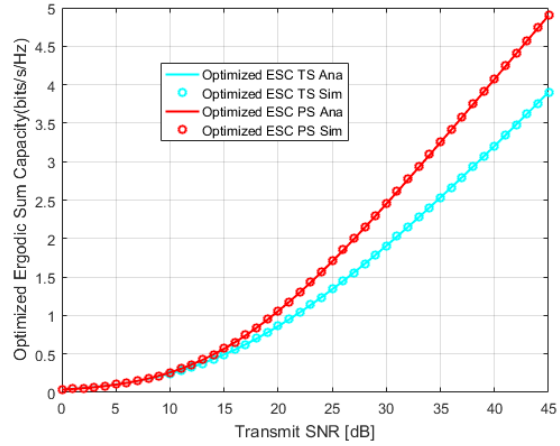

Fig. 7. Optimized Ergodic Sum Capacity

over the Rayleigh fading channels, in which one source or base station (BS) transmits symbols to two destination nodes through the direct link and with the help of EH based relay node. Therefore, for the considered NOMA-SWIPT system with the direct link, we investigated the EC and ESC of the TS, PS relaying architecture with NOMA. We derived the analytical expressions for the EC and the ESC and validated it through the simulation results, which showed that our derived analytical expressions are intact. We also provided a thorough comparison of the TS and PS relaying with NOMA for the considered system model. Our results confirmed that, through the optimal choice of the power splitting factor ϵ, it is possible to achieve better optimized ESC for the PS relaying with NOMA than the TS relaying with NOMA.

In this work, we only investigated the single signal detection at the UE_1 and UE_2. Since the direct link is also involved, use of maximal ratio combining (MRC) at the receiving node UE_1 and UE_2 will further increase the ESC of the considered system model with the direct link. For the future work, we would like to show further performance improvement through MRC on the ESC and compare it with the current work and conventional orthogonal multiple access schemes.

REFERENCES

[1] A. Ijaz, L. Zhang, M. Grau, A. Mohamed, S. Vural, A. U. Quddus, M. A. Imran, C. H. Foh, and R. Tafazolli, "Enabling massive iot in 5g and beyond systems: Phy radio frame design considerations," *IEEE Access*, vol. 4, pp. 3322–3339, 2016.

[2] S. Islam, M. Zeng, O. A. Dobre, and K.-S. Kwak, "Non-orthogonal multiple access (noma): How it meets 5g and beyond," *arXiv preprint arXiv:1907.10001*, 2019.

[3] L. Dai, B. Wang, Z. Ding, Z. Wang, S. Chen, and L. Hanzo, "A survey of non-orthogonal multiple access for 5g," *IEEE communications surveys & tutorials*, vol. 20, no. 3, pp. 2294–2323, 2018.

[4] Z. Ding, X. Lei, G. K. Karagiannidis, R. Schober, J. Yuan, and V. K. Bhargava, "A survey on non-orthogonal multiple access for 5g networks: Research challenges and future trends," *IEEE Journal on Selected Areas in Communications*, vol. 35, no. 10, pp. 2181–2195, 2017.

[5] S. R. Islam, N. Avazov, O. A. Dobre, and K.-S. Kwak, "Power-domain non-orthogonal multiple access (noma) in 5g systems: Potentials and challenges," *IEEE Communications Surveys & Tutorials*, vol. 19, no. 2, pp. 721–742, 2016.

[6] X. Su, A. Castiglione, C. Esposito, and C. Choi, "Power domain noma to support group communication in public safety networks," *Future Generation Computer Systems*, vol. 84, pp. 228–238, 2018.

[7] C. Moraes and D. Har, "Charging distributed sensor nodes exploiting clustering and energy trading," *IEEE Sensors Journal*, vol. 17, no. 2, pp. 546–555, 2016.

[8] X. Li, C. Luo, H. Ji, Y. Zhuang, H. Zhang, and V. C. Leung, "Energy consumption optimization for self-powered iot networks with non-orthogonal multiple access," *International Journal of Communication Systems*, p. e4174, 2019.

[9] M. Vaezi, G. Amarasuriya, Y. Liu, A. Arafa, F. Fang, and Z. Ding, "Interplay between noma and other emerging technologies: A survey," *arXiv preprint arXiv:1903.10489*, 2019.

[10] A. A. Nasir, X. Zhou, S. Durrani, and R. A. Kennedy, "Relaying protocols for wireless energy harvesting and information processing," *IEEE Transactions on Wireless Communications*, vol. 12, no. 7, pp. 3622–3636, July 2013.

[11] M. B. Uddin, M. F. Kader, and S. Y. Shin, "Uplink cooperative diversity using power-domain nonorthogonal multiple access," *Transactions on Emerging Telecommunications Technologies*, p. e3678, 2019.

[12] A. Rauniyar, P. Engelstad, and O. Østerbø, "Rf energy harvesting and information transmission based on noma for wireless powered iot relay systems," *Sensors*, vol. 18, no. 10, p. 3254, 2018.

[13] A. Rauniyar, P. E. Engelstad, and O. N. Østerbø, "Performance analysis of rf energy harvesting and information transmission based on noma with interfering signal for iot relay systems," *IEEE Sensors Journal*, vol. 19, no. 17, pp. 7668–7682, Sep. 2019.

[14] J.-B. Kim and I.-H. Lee, "Non-orthogonal multiple access in coordinated direct and relay transmission," *IEEE Communications Letters*, vol. 19, no. 11, pp. 2037–2040, 2015.

[15] J.-B. Kim, I.-H. Lee, and J. Lee, "Capacity scaling for d2d aided cooperative relaying systems using noma," *IEEE Wireless Communications Letters*, vol. 7, no. 1, pp. 42–45, 2017.

[16] H. Liu, Z. Ding, K. J. Kim, K. S. Kwak, and H. V. Poor, "Decode-and-forward relaying for cooperative noma systems with direct links," *IEEE Transactions on Wireless Communications*, vol. 17, no. 12, pp. 8077–8093, 2018.

[17] D.-B. Ha and S. Q. Nguyen, "Outage performance of energy harvesting df relaying noma networks," *Mobile Networks and Applications*, vol. 23, no. 6, pp. 1572–1585, 2018.

[18] C. Zhong, H. A. Suraweera, G. Zheng, I. Krikidis, and Z. Zhang, "Improving the throughput of wireless powered dual-hop systems with full duplex relaying," in *2015 IEEE International Conference on Communications (ICC)*. IEEE, 2015, pp. 4253–4258.

[19] Y. Ye, Y. Li, D. Wang, and G. Lu, "Power splitting protocol design for the cooperative noma with swipt," in *2017 IEEE International Conference on Communications (ICC)*. IEEE, 2017, pp. 1–5.

[20] I. S. Gradshteyn and I. M. Ryzhik, *Table of integrals, series, and products*. Academic press, 1980.